Draft version February 15, 2012
Preprint typeset using LaTeX style emulateapj v. 5/2/11

A COMPLETE SAMPLE OF BRIGHT *SWIFT* LONG GAMMA-RAY BURSTS I: SAMPLE PRESENTATION, LUMINOSITY FUNCTION AND EVOLUTION

R. Salvaterra,[1] S. Campana[2], S.D. Vergani[2,3] S. Covino[2] P. D'Avanzo[2] D. Fugazza[2] G. Ghirlanda[2] G, Ghisellini[2] A. Melandri[2] L. Nava[4] B. Sbarufatti[2] H. Flores[3] S. Piranomonte[5] G. Tagliaferri[2]

Draft version February 15, 2012

ABSTRACT

We present a carefully selected sub-sample of *Swift* Long Gamma-ray Bursts (GRBs), that is complete in redshift. The sample is constructed by considering only bursts with favorable observing conditions for ground-based follow-up searches, that are bright in the 15-150 keV *Swift*/BAT band, i.e. with 1-s peak photon fluxes in excess to 2.6 ph s^{-1} cm^{-2}. The sample is composed by 58 bursts, 52 of them with redshift for a completeness level of 90%, while another two have a redshift constraint, reaching a completeness level of 95%. For only three bursts we have no constraint on the redshift. The high level of redshift completeness allows us for the first time to constrain the GRB luminosity function and its evolution with cosmic times in a unbiased way. We find that strong evolution in luminosity ($\delta_l = 2.3 \pm 0.6$) or in density ($\delta_d = 1.7 \pm 0.5$) is required in order to account for the observations. The derived redshift distribution in the two scenarios are consistent with each other, in spite of their different intrinsic redshift distribution. This calls for other indicators to distinguish among different evolution models. Complete samples are at the base of any population studies. In future works we will use this unique sample of *Swift* bright GRBs to study the properties of the population of long GRBs.

Subject headings: gamma–ray: burst – stars: formation – cosmology: observations.

1. INTRODUCTION

Gamma-ray bursts are powerful flashes of high–energy photons occurring at an average rate of a few per day throughout the Universe. They are detected at all redshifts, from the local Universe up to the extreme high redshifts (Salvaterra et al. 2009; Tanvir et al. 2009; Cucchiara et al. 2011a). Our knowledge of the distribution of long GRBs through cosmic times is still hampered by the fact that most of the observed *Swift* GRBs are without redshift. Indeed, the measure of the distance has been secured for only $\sim 1/3$ of the cases. Given the low completeness level in redshift determination, the effect of possible observational biases could be important in shaping their redshift distribution (Fiore et al. 2007). This fact strongly limit the possibility of well grounded statistical studies of the rest-frame properties of long GRBs and their evolution with cosmic time. Therefore, it is of paramount importance to obtain an unbiased complete sample of GRBs, capable to fully represent this class of object.

To this end, we present in this paper a well selected sub-sample of the full *Swift* database. We select bursts that have favorable observing conditions for redshift determination from ground and that are bright in the 15-150 keV *Swift*/BAT band. We find 58 bursts matching our selection criteria with a completeness level in redshift determination of 90%. The completeness level increases up to $\sim 95\%$ by considering the redshift constraints imposed by the detection of the afterglow or host galaxy in some optical filters. Therefore, our selection criteria allow us to construct a sizable sample of long bursts that is (almost) complete in redshift, providing the solid basis for the study of the long GRB population in an unbiased way. In particular, since our selection is based on the brightness in the *Swift*/BAT band, our sample is not biased against the detection of dark bursts, thus providing a complete description of the whole long GRB population.

In the present paper, we will take advantage of the high completeness level of our sample to constrain the GRB luminosity function (LF) and its evolution with cosmic time. In the last few years, this problem has been faced by many different authors ((e.g. Porciani & Madau 2001, Firmani et al. 2004, Guetta et al. 2005, Natarajan et al. 2005, Daigne et al. 2006, Salvaterra & Chincarini 2007, Salvaterra et al. 2009b, Butler et al. 2010, Wanderman & Piran 2010, Campisi et al. 2010, Qin et al. 2010, Virgili et al. 2011, Robertson & Ellis 2012). There is a general agreement about the fact that GRBs must have experienced some sort of evolution through cosmic time, whereas the nature and the level of such evolution is still matter of debate. Most of the previous works relied on the assumption that bursts lacking of redshift measurements follow closely the redshift distribution of bursts with known z. In the past, we tried to overcome this assumption by deriving conservative lower limit on the level of evolution on the basis of the number of bursts detected at $z > 2.5$ (Salvaterra & Chincarini 2007) and of bursts with peak luminosity $L > 10^{53}$ erg s^{-1} (Salvaterra et al. 2009b). For the first time, thanks to our well selected, complete sub-sample of *Swift* GRBs, we

[1] INAF, IASF Milano, via E. Bassini 15, I-20133 Milano, Italy, ruben@lambrate.inaf.it
[2] INAF, Osservatorio Astronomico di Brera, via E. Bianchi 46, I-23807 Merate (LC), Italy
[3] Laboratoire GEPI, Observatoire de Paris, CNRS-UMR8111, Univ. Paris-Diderot 5 place Jules Janssen, 92195 Meudon, France
[4] SISSA, via Bonomea 265, I-34136 Trieste, Italy
[5] INAF, Osservatorio Astronomico di Roma, Via Frascati 33, 00040, Monte Porzio Catone, Rome, Italy

can tackle this issue in a unbiased way. In future works we will use this sample to study the correlation between physical parameters of the bursts, the properties of the burst light curves and of the environment in which they explode.

This paper is organized as follow. In Sect. 2 we describe our selection criteria and present our sample. We present our models of the GRB LF and redshift distribution in Sect. 3, while the results are given in Sect. 4. We extrapolate our findings to the detection limit of *Swift* in Sect. 5. Finally, in Sect. 6 we draw our conclusions.

2. THE SAMPLE

About 1/3 of all GRBs observed by the *Swift* satellite (Gehrels et al. 2004) has a measured redshift. While this represents an enormous improvement with respect to the pre-*Swift* situation, the sample is still far to be considered as complete. Jakobsson et al. (2006) proposed a series of criteria in order to carefully select long GRBs which have observing conditions favorable for redshift determination. In particular, they required that: i) the burst has been well localized by *Swift*/XRT and its coordinate quickly distributed; ii) the Galactic extinction in the burst direction is low ($A_V < 0.5$); iii) the GRB declination is $-70^\circ < \delta < 70^\circ$; iv) the Sun-to-field distance is $\theta_{\rm Sun} > 55^\circ$; v) no nearby bright stars is present. While none of the above criteria is expected to alter significantly the redshift distribution of observed GRBs, the completness level is increased to $\sim 53\%$[6]. Still this level of completeness is way too low to permit robust population studies.

In order to construct a more complete sample we restrict ourself to GRBs that are relatively bright in the 15-150 keV *Swift*/BAT band. In particular, we select bursts matching the above criteria and having 1-s peak photon flux $P \geq 2.6$ ph s^{-1} cm^{-2}. This corresponds to an instrument that is ~ 6 times less sensitive than *Swift*. 58 GRBs match our selection criteria and are listed in Table 1 up to May 2011. 52 of them have measured redshift so that our completeness level is 90%. Of these 52, all but two (namely GRB 070521; Perley et al. 2009 and GRB 080602; Rossi et al. 2012) have spectroscopic confirmed redshift either from absorption lines over-imposed on the GRB optical afterglow or from emission lines of the GRB host galaxy. Moreover, for 3 of the 6 bursts lacking measured z the afterglow or the host galaxy have been detected in at least one optical filter, so that $\sim 95\%$ of the bursts in our sample have a constrained redshift. We note that, while our sample represents only $\sim 10\%$ of the full *Swift* sample, it contains more than 30% of long GRBs with known redshift.

The redshift distribution of the bursts in our sample is shown in Fig. 1. In spite of the rather severe cut in the observed photon flux, the bursts in our sample have a broad distribution in redshift. The mean (median) redshift of the sample is 1.84 ± 0.16 (1.64 ± 0.10) with a long tail at high-z extending, at least, up to $z = 5.47$.

3. MODEL DESCRIPTION

The expected redshift distribution of GRBs can be computed once the GRB LF and the GRB formation history has been specified. We briefly recap here the adopted formalism and refer the interested reader to Salvaterra & Chincarini (2007) and Salvaterra et al. (2009b) for the model details.

The observed peak photon flux, P, in the energy band $E_{\rm min} < E < E_{\rm max}$, emitted by an isotropically radiating source at redshift z is

$$P = \frac{(1+z)\int_{(1+z)E_{\rm min}}^{(1+z)E_{\rm max}} S(E)dE}{4\pi d_L^2(z)}, \quad (1)$$

where $S(E)$ is the differential rest–frame photon luminosity of the source, and $d_L(z)$ is the luminosity distance. To describe the typical burst spectrum we adopt a Band function with low- and high-energy spectral index -1 and -2.25, respectively (Band et al. 1993; Preece et al. 2000; Kaneko et al. 2006). The spectrum normalisation is obtained by imposing that the isotropic–equivalent peak luminosity is $L = \int_{1\,{\rm keV}}^{10000\,{\rm keV}} ES(E)dE$. In order to broadly estimate the peak energy of the spectrum, E_p, for a given L, we assumed the validity of the correlation between E_p and L (Yonetoku et al. 2004; Ghirlanda et al. 2005, Nava et al. 2011).

Given a normalised GRB LF, $\phi(L)$, the observed rate of bursts with peak flux between P_1 and P_2 is

$$\frac{dN}{dt}(P_1 < P < P_2) = \int_0^\infty dz \frac{dV(z)}{dz}\frac{\Delta\Omega_s}{4\pi}\frac{\Psi_{\rm GRB}(z)}{1+z} \times \int_{L(P_1,z)}^{L(P_2,z)} dL'\phi(L'), \quad (2)$$

where $dV(z)/dz = 4\pi c d_L^2(z)/[H(z)(1+z)^2]$ is the comoving volume element[7], and $H(z) = H_0[\Omega_M(1+z)^3 + \Omega_\Lambda + (1-\Omega_M-\Omega_\Lambda)(1+z)^2]^{1/2}$. $\Delta\Omega_s$ is the solid angle covered on the sky by the survey, and the factor $(1+z)^{-1}$ accounts for cosmological time dilation. Finally, $\Psi_{\rm GRB}(z)$ is the comoving burst formation rate.

We explore two general expression for the GRB LF: a single power-law with an exponential cut-off at low luminosity (exponential LF) and a broken power-law LF. The former is described by:

$$\phi(L) \propto \left(\frac{L}{L_{\rm cut}}\right)^{-\xi_b} \exp\left(-\frac{L_{\rm cut}}{L}\right), \quad (3)$$

and the latter by:

$$\phi(L) \propto \begin{cases} \left(\frac{L}{L_{\rm cut}}\right)^{-\xi_f} & \text{for } L \leq L_{\rm cut} \\ \left(\frac{L}{L_{\rm cut}}\right)^{-\xi_b} & \text{for } L > L_{\rm cut}, \end{cases} \quad (4)$$

where $L_{\rm cut}$ is the cut-off (break) luminosity and ξ_b and ξ_f are the bright- and faint-end power-law index, respectively. The GRB LF are normalized to unity. In order to prevent the integral to diverge we adopt a minimum GRB luminosity $L_{\rm min} = 10^{49}$ erg s^{-1}. We test that our results do not change if minimum luminosity of 10^{48} erg

[6] Up to May 2011, the sample consists in 248 long GRBs, 132 with measured redshift. See http://www.raunvis.hi.is/∼pja/GRBsample.html

[7] We adopted the 'concordance' model values for the cosmological parameters: $h = 0.7$, $\Omega_m = 0.3$, and $\Omega_\Lambda = 0.7$.

GRB	redshift	ref.	GRB	redshift	ref	GRB	redshift	ref	GRB	redshift	ref
050318	1.44	1	061007	1.26	2	080603B	2.69	2	090709A	< 3.5	15
050401	2.90	2	061021	0.35	2	080605	1.64	2	090715B	3.00	16
050416A	0.65	3	061121	1.31	2	080607	3.04	2	090812	2.45	17
050525A	0.61	4	061222A	2.09	3	080613B	-	-	090926B	1.24	18
050802	1.71	2	070306	1.50	2	080721	2.59	2	091018	0.97	19
050922C	2.20	2	070328	$< 4^{(c)}$		080804	2.20	2	091020	1.71	20
060206	4.05	2	070521	1.35	3	080916A	0.69	2	091127	0.49	21
060210	3.91	2	071020	2.15	2	081007	0.53	8	091208B	1.06	22
060306	$3.5^{(a)}$		071112C	0.82	2	081121	2.51	9	100615A	-	-
060614	0.13	2	071117	1.33	2	081203A	2.10	10	100621A	0.54	23
060814	$1.92^{(b)}$		080319B	0.94	2	081221	$2.26^{(a)}$		100728B	2.106	24
060904A	-	-	080319C	1.95	2	081222	2.77	11	110205A	2.22	25
060908	1.88	2	080413B	1.1	2	090102	1.55	12	110503A	1.613	26,27
060912A	0.94	5	080430	0.77	6	090201	< 4	13			
060927	5.47	2	080602	$\sim 1.4^{(d)}$	7	090424	0.54	14			

Table 1
List of the bursts matching our selection criteria. Redshifts or limits are provided in the following references: [1] Berger et al. 2005, [2] Fynbo et al. 2009a and references therein, [3] Perley et al. 2009, [4] Foley et al. 2005, [5] Levan et al. 2007, [6] Cucchiara & Fox 2008, [7] Rossi et al. 2012, [8] Berger et al. 2008, [9] Berger & Rauch 2008, [10] Kuin et al. 2009, [11] Cucchiara et al. 2008, [12] de Ugarte Postigo et al. 2009a, [13] D'Avanzo et al. 2009, [14] Chornock et al. 2009, [15] Perley et al. in prep., [16] Wiersema et al. 2009a, [17] de Ugarte Postigo et al. 2009b, [18] Fynbo et al. 2009b, [19] Chen et al. 2009, [20] Xu et al. 2009, [21] Cucchiara et al. 2009, [22] Wiersema et al. 2009b, [23] Milvang-Jensen et al. 2010, [24] Flores et al. 2010, [25] Cucchiara et al. 2011b, [26] de Ugarte Postigo et al. 2011, [27] D'Avanzo et al. 2011.

(a) based on VLT/X-shooter spectra of the host galaxies obtained within the program 087.A-0451 (PI: H. Flores). The spectra were reduced using the X-shooter data reduction pipeline version 1.3.7 (see Goldoni et al. 2006). In the NIR arm spectrum of GRB 060306 we identified at the afterglow position the [OII] doublet emission at $z = 3.5$, while in the NIR arm spectrum of GRB 081221 the [OIII] and Hα emission lines are present at $z = 2.26$ at the afterglow position.
(b) for this GRB a redshift of $z = 0.84$ was reported by Thoene et al, (2007). Images and spectra at the afterglow position have been taken also using the VLT/FORS within the program 177.A-0591 (PI: J. Hjorth). We downloaded these data from the ESO Archive and reduced them with standard procedures using the ESO-MIDAS package. At the afterglow position we could identify an object, showing a continuum signature in the spectra, that we therefore consider to be the host galaxy of GRB 060814. We can also identify the galaxy reported by Thoene et al. (2007), at $z = 0.84$, but this object is offset from the afterglow position. VLT/X-shooter spectroscopy of the host galaxy has been performed within the program 084.A-0303 (PI: J. Fynbo). We reduced these spectra using the X-shooter data reduction pipeline version 1.2.0 (see Goldoni et al. 2006). Thanks to the identification in the NIR arm of the [OII] doublet, [OIII] λ5007 and Hα emission lines associated with the host galaxy, we can establish a redshift of $z = 1.92$ for GRB 060814.
(c) based on the $R-$band host galaxy detection in ESO-VLT/FORS2 imaging data obtained within the program 177.A-0591 (PI: J. Hjorth), taken from the ESO Archive.
(d) photometric redshift on the bases of the most probable host galaxy association in the XRT error circle (Rossi et al. 2012).

s^{-1} is adopted (apart from the value of the normalization η_0).

4. MODEL RESULTS

We optimize the value of the model free parameters, that is the GRB LF, the normalization η_0 and the evolution parameter, by minimizing the C-stat function (Cash 1979) jointly fitting the observed differential number counts in the 50–300 keV band of BATSE (Stern et al. 2001, 2002) and the observed redshift distribution of bursts in our sample with photon fluxes in excess to 2.6 ph s^{-1} cm^{-2} in the *Swift* 15-150 keV band[8]. For BATSE, we adopt 9.1 yrs of observation with an average exposure factor of 0.47, including both Earth-blocking and average duty cycle for useful 1.024s continuos record (Stern et al. 2002). While our complete *Swift* sample provides a powerful test for the existence and the level of evolution of the long GRB population with redshift, the fit to the BATSE number counts allows us to obtain the present day GRB rate density and to better constrain the GRB LF free parameters. It is worth to note that the best-fit parameters provide a good fit also of the *Swift* differential peak-flux number counts once the 15-150 keV band, the FOV of 1.4sr and the observing lifetime of *Swift* are considered (see also Salvaterra & Chincarini 2007). The best fit parameter values together with their 1-σ confidence level[9] for different models are provided in Table 2. The corresponding redshift distributions for bursts with $P > 2.6$ ph s^{-1} cm^{-2} are shown in Fig. 1. We test for each model the two different GRB LF parametrizations described in the previous section and we report in Fig. 1 the one that gives the best result.

4.1. *No-evolution model*

In a first simple (no-evolution) scenario we can assume that long GRBs traces the cosmic star formation and that their LF is constant in redshift ($L_{\rm cut}(z) = L_{\rm cut,0}$). In this case the cosmic GRB formation rate is $\Psi_{\rm GRB}(z) =$

[8] For those GRBs lacking of redshift measurement, we randomly assign a redshift from a flat z-distribution (taking into account the available redshift constraints) not to introduce any a-priori bias. We produced 1000 of such random realizations.

[9] The errors at 1-σ confidence level on the parameters of interest (GRB LF and evolution parameter) adopting a C-stat increment of 2.30, 3.53 and 4.72 for 2, 3, and 4 parameters of interest, respectively.

Model	evo. par.	η_0	$L_{0,51}$	ξ_f	ξ_b	C-stat	AIC
cut-off luminosity function							
no evolution	-	0.30	$1.0^{+0.9}_{-0.5}$	-	$2.03^{+0.16}_{-0.12}$	93	99
luminosity	$\delta_l = 2.3 \pm 0.6$	0.14	$0.22^{+0.27}_{-0.13}$	-	$2.02^{+0.13}_{-0.10}$	27	35
density	$\delta_n = 1.6 \pm 0.4$	0.03	$3.07^{+3.29}_{-1.94}$	-	$2.09^{+0.23}_{-0.17}$	38	46
metal	$Z_{\rm th} = 0.14 \pm 0.16$	0.04	$4.4^{+5.6}_{-2.8}$	-	$2.19^{+0.30}_{-0.20}$	37	45
double power-law luminosity function							
no evolution	-	2.06	25^{+68}_{-21}	$1.56^{+0.11}_{-0.42}$	$2.31^{+0.35}_{-0.31}$	88	96
luminosity	$\delta_l = 2.1 \pm 0.6$	0.21	$0.55^{+0.69}_{-0.34}$	$0.74^{+1.42}_{-1.36}$	$1.92^{+0.14}_{-0.11}$	33	43
density	$\delta_n = 1.7 \pm 0.5$	0.24	38^{+63}_{-27}	$1.50^{+0.16}_{-0.32}$	$2.32^{+0.77}_{-0.32}$	27	37
metal	$Z_{\rm th} = 0.10 \pm 0.18$	0.41	47^{+75}_{-35}	$1.45^{+0.17}_{-0.35}$	$2.58^{+0.60}_{-0.50}$	26	36

Table 2
Best fit parameters for different models. Errors show the 1-σ confidence level for the parameters of interest (see text in section 4 for the details). The last two column report the total C-stat value (i.e. the sum of the C-stat values obtained from the fit of the BATSE and *Swift* dataset) and the Akaike Information Criterion (AIC) score, respectively. We note that in order to properly compare different models the AIC criterion has to be considered, where $\exp((\mathrm{AIC_{min}} - \mathrm{AIC}_i)/2)$ can be interpreted as the relative probability that the i-th model minimizes the (estimated) information loss with respect to the model with the minimum AIC, $\mathrm{AIC_{min}}$. The total number of data points in the fit is 33. The GRB formation rate at $z = 0$, η_0, is given in units of $\mathrm{Gpc^{-3}\ yr^{-1}}$ and the characteristic luminosity $L_{0,51}$ is units of 10^{51} erg $\mathrm{s^{-1}}$.

$\eta_0 \Psi_\star(z)$, where $\Psi_\star(z)$ is the normalized cosmic star formation rate (SFR) and η_0 is the present-day GRB formation rate density in units of $\mathrm{Gpc^{-3}\ yr^{-1}}$. We adopt the cosmic SFR recently computed by Li (2008) that extended the previous work by Hopkins & Beacom (2006) to higher redshifts.

This no-evolution scenario (dashed line in Fig. 1) clearly does not provide a good representation of the observed redshift distribution of our sample, confirming previous findings (e.g. Daigne et al. 2006, Salvaterra & Chincarini 2007, Salvaterra et al. 2009b, Qin et al. 2010, Wanderman & Piran 2010, Virgili et al. 2011). In particular, the peak of the GRB redshift distribution is at lower redshift than observed and consequently the rate of GRBs at high-z is underpredicted. This is confirmed by a more detailed statistical analysis. Indeed, on the basis of the Akaike information criterion (Akaike 1974) we can safely discard this model being $\sim 10^{-14}$ times as probable as the luminosity evolution model to minimize the information loss (the density evolution model with the broken power-law LF is 0.24 as probable as the luminosity one with the cut-off LF). Moreover, a KS test between the no evolution best-fit model and the data of our sample gives a chanche probability of $\sim 5 \times 10^{-5}$ that the two distribution are drawn from the same parent population.

In the following sections, we will consider evolution scenarios that may enhance the number of detections at high-z. In particular, we explore: i) a luminosity evolution model in which high-z GRB are typically brighter than low-z bursts and, ii) two density evolution models, both leading to an enhancement of the GRB formation rate with redshift. Hybrid models, with both luminosity and density evolution, are in principle possible. However, the fit with hybrid models results to be very degenerate and does not provide usefull constraints. Therefore, we prefer here to consider the two scenarios separately to highlight possible similarities/differences between the two kinds of evolution.

4.2. *Luminosity evolution model*

Evolution in the GRB LF can provide an enhancement of the high-z GRB detection, representing a viable way to reconcile model results with the observations. Here, we consider the possibility that the cut-off (break) luminosity is an increasing function of the redshift, that is $L_{\rm cut}(z) = L_{\rm cut,0}(1+z)^{\delta_l}$. We find that a strong luminosity evolution with $\delta_l = 2.3 \pm 0.6$ is required to reproduce the observed redshift distribution of the bursts in our complete sample (light shaded area in Fig. 1). The result does not depend on the assumed expression of the GRB LF.

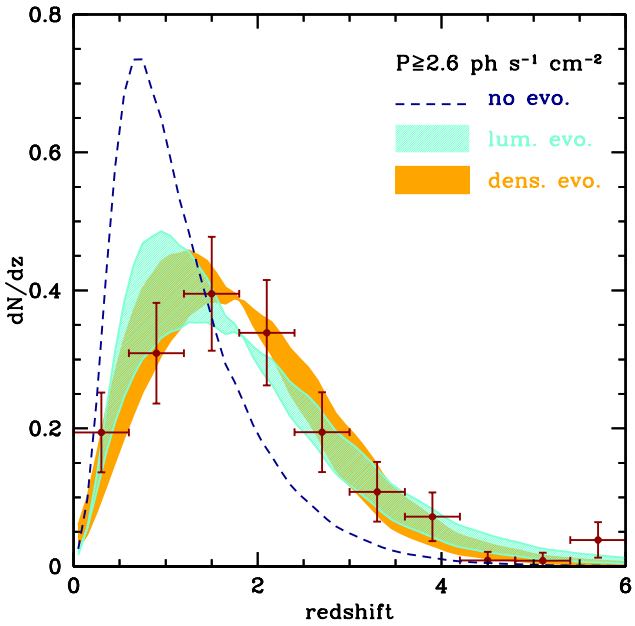

Figure 1. Normalized redshift distribution of GRBs with $P \geq 2.6$ ph $\mathrm{s^{-1}\ cm^{-2}}$. Data points (red) show the observed redshift distribution and the error bars show the Poisson uncertainties on the number of detection in the redshift bin. The dashed line (blue) shows the expected distribution for the no-evolution case. Results of luminosity and density evolution models are shown with the light blue and dark shaded orange regions, respectively, taking into account the errors on the evolution parameter. (A color version of this figure is available in the online journal.)

4.3. *Density evolution models*

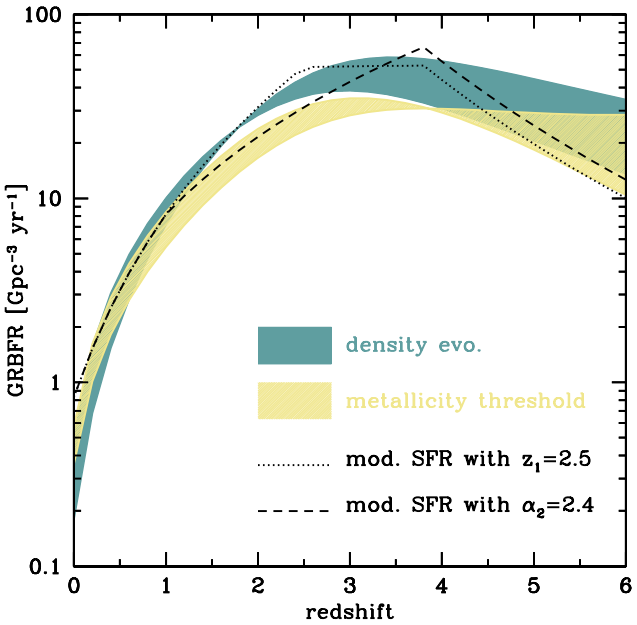

Figure 2. Intrinsic redshift distribution of long GRBs for different density evolution models. Dark blue and light yellow shaded areas show the results for the density evolution model and for the metallicity threshold model, respectively. Dotted (dashed) lines reports the modified SFR with $z_1 = 2.5$ ($\alpha_2 = 2.4$). In all cases, no evolution of the GRB LF has been assumed. (A color version of this figure is available in the online journal.)

An increase of the rate of GRB formation with redshift (on the top of the known evolution of the SFR density) will also lead to an enhanced detection of bursts at high-z. As a general case, we parametrize the evolution in the GRB formation rate as $\eta(z) = \eta_0(1+z)^{\delta_n}$. By fitting our datasets we find that strong density evolution is required with $\delta_n = 1.7 \pm 0.5$. The amount of evolution does not depend on the assumed expression of the GBR LF. However, we note that the cut-off LF tends to underestimate the number of low-z bursts with respect to the observed one, leading to some discrepancy with the first data point.

The large value of δ_n implies an important shift of the peak of the GRB formation rate towards higher redshifts with respect to stars. We further investigate this issue by applying a "correction" to the shape of the cosmic SFR. This is usually parametrized as three power-laws (Hopkins & Beacom 2006, Li 2008) with power-index $\alpha_1 = 3.3$, $\alpha_2 = 0.055$, $\alpha_3 = -4.46$ and breaks at $z_1 = 0.993$ and $z_2 = 3.8$ (Li 2008). We fit our datasets by letting one of the above parameters free to vary in addition to those describing the GRB LF. We find that the observed redshift distribution of bursts in our sample can be explained either by an increase of the redshift of the first break to $z_1 = 2.5 \pm 0.5$ or by a hardening of the second power-law to $\alpha_2 = 2.4 \pm 0.4$. In both cases, the GRB formation rate is found to peak at a much higher redshift with respect to stars. The intrinsic redshift distribution of GRBs is shown in Fig. 2.

4.4. *Metallicity threshold models*

A subclass of density evolution models foresee the formation of long GRBs preferentially in low-metallicity environments. In this case GRBs will be biased tracers of the star formation activity being their formation suppressed at low-z where most of the galaxies are relatively metal-rich. Following Langer & Norman (2006), we model the fractional mass density belonging to metallicity below a given threshold, $Z_{\rm th}$ as

$$\Sigma(z) = \frac{\hat{\Gamma}(0.84, (Z_{\rm th}/{\rm Z}_\odot)^2 10^{0.3z})}{\Gamma(0.84)}, \qquad (5)$$

where $\hat{\Gamma}$ (Γ) are the incomplete (complete) gamma function, and $\Gamma(0.84) \simeq 1.122$. The GRB formation rate is then given by $\Psi_{\rm GRB}(z) \propto \Sigma(z)\Psi_\star(z)$.

We fit our datasets letting $Z_{\rm th}$ free to vary. The available data are well described by models with $Z_{\rm th} \leq 0.3$ Z$_\odot$, almost independently on the assumed LF. The resulting LF is similar to the one obtained for density evolution model. Indeed, the two predicted redshift distributions match each others within the uncertainties and we refer to the dark shaded curves in Fig. 1 also for the metallicity threshold model.

The range of values for $Z_{\rm th}$ found in our analysis is in agreement with the expectation of the collapsar model (Woosley & Heger 2006; Fryer et al. 1999). However, such strong metallicity cut-offs seem to be inconsistent with the observed properties of GRB host at $z < 1$ (Mannucci et al. 2011; Kocevski et al. 2011; Campisi et at. 2011a). In particular, Campisi et al. (2011a) have shown that in the presence of a strong metallicity cut-off for the GRB progenitor star, the expected distribution of GRB host galaxies in the M-Z and Fundamental Metallicity Relation planes is much flatter than observed. Larger metallicity thresholds will require some luminosity evolution in order to reproduce the available data. For $Z_{\rm th} = 0.5$ Z$_\odot$, the typical burst luminosity should increase with redshift as $(1+z)^{1.3\pm0.6}$.

5. *SWIFT* REDSHIFT DISTRIBUTION

We compute the redshift distribution expected for the full *Swift* dataset assuming a photon flux limit of $P = 0.4$ ph s^{-1} cm^{-2} and fixing the model free parameters to the values given in Table 2. The results are shown in Fig. 3 for the different evolution scenarios here explored. The models are compared with the redshift distribution inferred from the sample of GRBs observed by GROND (Greiner et al. 2011). This sample has a completeness level similar to our but is smaller in size and cover a broader redshift range. We find that our evolution models provide a good description of the observed redshift distribution of the GROND sample without the need of any adjustment of the free paramters (a KS test gives a probability of 50%), whereas the no evolution model is excluded (probability of 5×10^{-4}). This further confirms the reliability of our analysis strenghtening our conclusions.

The predicted redshift distribution of bursts detectable by *Swift* presents a steep raise at low-z peaking at $z \sim 2$ with a tail extending at higher redshifts. The median redshift of the distribution is $z = 2.05 \pm 0.15$ where the error takes into account the uncertainties on the evolution parameters. We predict that $3-5\%$ of the bursts lie at $z > 5$, consistently with the observational estimate of $5.5 \pm 2.8\%$ (Greiner et al. 2011). This further confirms that the majority of dark GRBs are not high-z sources but more likely obscured by dust (Perley et al. 2009,

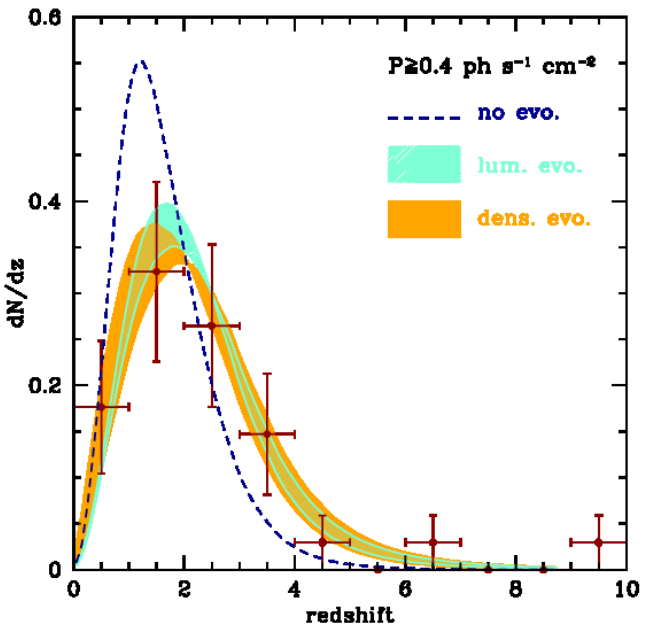

Figure 3. Normalized redshift distribution of GRBs detectable with *Swift*, i.e. with observed photon flux in excess to $P_{\rm lim} = 0.4$ ph s^{-1} cm^{-2}. The data show the observed redshift distribution as reported by Greiner et al. (2011), on the basis of the almost complete sample of GRBs detected by GROND. Error bars show the Poisson uncertainties on the number of objects in the redshift bin. Model results are shown as in Fig. 1. No attempt to fit the observed redshift distribution has been done. (A color version of this figure is available in the online journal.)

Greiner et al. 2011). At $z > 8$, we expect $1.3 - 3.5$ GRBs[10] among the 530 *Swift* GRBs. This is consistent with the two detections reported so far, i.e. GRB 090423 at $z = 8.2$ (Salvaterra et al. 2009; Tanvir et al. 2009) and GRB 090429B at $z \sim 9.4$ (Cucchiara et al. 2011).

It is worth to note that the two evolution scenarios here explored predict very similar distributions. Therefore we can not distinguish between luminosity and density evolution simply on the basis of the *Swift* observed redshift distribution.

6. CONCLUSIONS

We select a sub-sample of *Swift* long GRBs that is complete in redshift. The sample is composed by bursts with favourable observing conditions and with 1-s peak photon fluxes $P \geq 2.6$ ph s^{-1} cm^{-2}. It contains 58 bursts with a completeness level of $\sim 90\%$ and provides the basis for statistical studies of the properties of long GRBs and their evolution with redshift in a unbiased way. GRBs can be used to study fundamental issues in astronomy and astrophysics, such as the star formation rate and the stellar and metal abundances evolution. They can be use as tracers of the galaxy evolution, of the ISM composition and to investigate the early universe. Complete and fully representative samples of GRBs are therefore unique tools to perform these investigations.

Here, we use the observed burst redshift distribution of our complete sample to probe and constrain the evolution of the long GRB population in redshift. We confirm that GRBs must have experienced some sort of evolution being more luminous or more numerous in the past than observed today. We found that in order to match the observed distribution, the typical burst luminosity should increase as $(1+z)^{2.3\pm0.6}$ or the GRB rate density as $(1+z)^{1.7\pm0.5}$ on the top of the known cosmic evolution of the SFR. This result does not depend on the assumed expression of the GRB luminosity function. We also explore models in which GRBs form preferentially in low-metallicity environments. We find that the metallicity threshold for GRB formation should be lower than 0.3 $Z_\odot$ in order to account for the observations assuming no evolution of the GRB LF. This value, while consistent with the expectations of collapsar models, seems to be at odd with the observed properties of $z < 1$ GRB hosts (Levesque et al. 2010; Mannucci et al. 2011; Campisi et al 2011a).

Extrapolating our results to $P = 0.4$ ph s^{-1} cm^{-2}, the predictions of evolution models are consistent with available observational constrain without the need of any adjustment of the model free parameters. We also note that the predicted redshift distributions at the sensitivity of *Swift* for different evolution models are very similar, implying that it would be extremely difficult to distinguish among different kind of evolutions only on the basis of the observed redshift distribution.

On the bases of our models we predict that $3-5\%$ of the bursts detected by *Swift* lie at $z > 5$ consistently with the most recent observational estimate of $5.5\pm2.8\%$ (Greiner et al. 2011). This indicates that high-z bursts can contribute only marginally to the observed fraction of dark bursts. Finally, we expect 30-50 bursts per year over the entire sky with luminosities in excess to 10^{53} erg s^{-1} and 2-5 with luminosities exceeding 10^{54} erg s^{-1}. Extreme luminous GRBs, such as the current *Swift* record holder GRB 080607 with $L_{iso} = 2.26\times10^{54}$ erg s^{-1} (Perley et al. 2011), should be rare, exploding once every 0.5-1 years in the Universe. This corresponds to one detection every $\sim 0.7-1.5$ years in the field of view of *Fermi*/GBM (and one every 5-12 years for *Swift*).

[10] We do not consider here the possible contribution of PopIII GRBs that may provide additional GRBs at very high-z (Campisi et al. 2011b; de Souza et al. 2011).

ACKNOWLEDGMENTS

We thank A. Rossi and D. Perley for sharing their results before publication. This work has been supported by ASI grant I/004/11/0.

REFERENCES

Akaike, H., 1974, ITAC, 19, 716
Band, D., Matteson, J., Ford, L. et al., 1993, ApJ, 413, 281
Berger, E., Kulkarni, S.R., Fox, D.B., et al., 2005, ApJ, 634, 501
Berger, E., Fox, D.B., Cucchiara, A., Cenko, S.B., 2008, GCN 8335
Berger, E. & Rauch, M., 2008, GCN 8542
Butler, N.R., Bloom, J.S., Poznanski, D., 2010, ApJ, 711, 495
Campisi, M.A, Li, L.-X., Jakobsson, P., 2010, MNRAS, 407, 1972
Campisi, M.A. Tapparello, C., Salvaterra, R., Mannucci, F., Colpi, M., 2011a, MNRAS, 417, 1013
Campisi, M.A., Maio, U., Salvaterra, R., Ciardi, B., 2011b, MNRAS, 416, 2760
Cash, W., 1979, ApJ, 228, 939
Chen, H.-W., Helsby, J., Shectman, S., Thompson, I., Craneet, J., 2009, GCN 10038
Chornock, R., Perley, D.A., Cenko, S.B., Bloom, J.S., 2009, GCN 9243
Cucchiara, A. & Fox, D.B., 2008 GCN 7654

Cucchiara, A., Fox, D.B., Cenko, S.B., Berger, E., 2008, GCN 8713
Cucchiara, A., Fox, D., Levan, A.J., Tanvir, N., 2009, GCN 10202
Cucchiara, A., Levan, A.J., Fox, D.B., et al., 2011a, ApJ, 736, 7
Cucchiara, A., Cenko, S.B., Bloom, A., et al., 2011b, ApJ, 743, 154
Daigne, F., Rossi, E. M., & Mochkovitch, R. 2006, MNRAS, 372, 1034
D'Avanzo, P., Thoene, C.C., Fugazza, D., et al., 2009, GCN 8873
D'Avanzo, P., D'Elia, V., Di Fabrizio, L., Gurtu, A., 2011, GCN 11997
de Souza, R.S., Yoshida, N., Ioka, K., 2011, A&A, 533, 32
de Ugarte Postigo, A., Jakobsson, P., Malesani, D., et al., 2009a, GCN 8766
de Ugarte Postigo, A., Gorosabel, J., Fynbo, J.P.U., Wiersema, K., Tanvir, N., 2009b, GCN 9771
de Ugarte Postigo, A., Castro-Tirado, A.J., Tello, J.C., Cabrera Lavers, A., Reverte, D., 2011, GCN 11993
Fiore, F., Guetta, D., Piranomonte, S., D'Elia, V., Antonelli, L. A., 2007, A&A, 470, 515
Firmani, C., Avila-Reese, V., Ghisellini, G., Tutukov, A.V., 2004, ApJ, 611, 1033
Flores, H., Fynbo, J.P.U., de Ugarte Postigo, A., et al., 2010, GCN 11317
Foley, R.J., Chen, H.-W., Bloom, J., Prochaska, J.X., 2005, GCN 3483
Fryer, C. L., Woosley, S. E., Hartmann, D. H., 1999, ApJ, 526, 152
Fynbo, J.P.U., Jakobsson, P., Prochaska, J.X., et al., 2009a, ApJS, 185, 526
Fynbo, J.P.U., Jakobsson, P., D'Elia, V., 2009b, GCN 9947
Gehrels, N., Chincarini, G., Giommi, P., et al. 2004, ApJ, 611, 1005
Ghirlanda, G., Ghisellini, G., Firmani, C., Celotti, A., Bosnjak, Z., 2005, MNRAS, 360, L45
Goldoni, P. et al., 2006, in Society of Photo-Optical Instrumentation Engineers (SPIE) Conference Series, Vol. 6269, Society of Photo-Optical Instrumentation Engineers (SPIE) Conference Series
Greiner, J., Kruehler, T., Klose, S., et al. 2011, A&A, 526, 30
Guetta, D., Piran, T. & Waxman, E., 2005, ApJ, 619, 412
Hopkins, A. M. & Beacom, J. F., 2006, ApJ, 651, 142
Kaneko, Y., Preece, R. D., Briggs, M. S., et al., 2006, ApJS, 166, 298
Kocevski, D. & West, A.A., 2011, ApJ, 735, 8
Kuin, N.P.M. et al. 2009, MNRAS, 395, 21
Jakobsson, P., Levan, A., Fynbo, J.P.U., et al., 2006, A&A, 447, 897
Langer, L. & Norman, C. A., 2006, ApJ, 638, L63
Levan, A.J., Jakobsson, P., Hurkett, C., et al., 2007, MNRAS, 378, 1439
Levesque, E.M., Kewley, L.J., Berger, E., Zahid, H. J., 2010, ApJ, 140, 1557
Li, L.-X., 2008, MNRAS, 388, 1487
Mannucci, F., Salvaterra, R., Campisi, M.A., 2011, MNRAS, 414, 1263
Milvang-Jensen, B., Goldoni, P., Tanvir, N.R., et al., 2010, GCN 10876
Nava, L., Salvaterra, R., Ghirlanda, G., et al., 2011, MNRAS in press, arXiv:1112.4470
Natarajan, P., Albanna, B., Hjorth, J., et al., 2005, MNRAS, 364, L8
Perley, D.A., Cenko, S.B., Bloom, J.S., et al., 2009, AJ, 138, 1690
Perley, D.A., Morgan, A.N., Updike, A., et al., 2011, AJ, 141, 36
Porciani, C. & Madau, P., 2001, ApJ, 548, 522
Preece, R. D., Briggs, M. S., Mallozzi, R. S., et al., 2000, ApJS, 126, 19
Qin, S.-F., Liang, E.-W., Lu, R.-J., Wei, J.-Y., Zhang, S.-N., 2010, MNRAS, 406, 558
Robertson, B.E. & Ellis R.S., 2012, ApJ, 744, 95
Rossi, A., Klose, S., Ferrero, P., et al., 2012, A&A submitted, arXiv:1202.1434
Salvaterra, R. & Chincarini, G., 2007, ApJ, 656, 49
Salvaterra, R., Della Valle, M., Campana, S., et al., 2009a, Nature, 461, 1258
Salvaterra, R., Guidorzi, C., Campana, S., Chincarini, G., Tagliaferri, G., 2009b, MNRAS, 396, 299
Stern, B.E., Tikhomirova, Y., Kompaneets, D., Svensson, R., Poutanen, J., 2001, ApJ, 563, 80
Stern, B.E., Atteia, J.-L., Hurley, K., 2002, ApJ, 578, 304
Tanvir, N.R., Fox, D.B., Levan, A.J., et al., 2009a, Nature, 461, 1254
Thoene, C., Perley, D.A., Bloom, J.S., 2007, GCN 6663
Virgili, F.J., Zhang, B., Nagamine, K., Choi, J.-H., 2011, MNRAS, 417, 3025
Wanderman, D. & Piran, T., 2010, MNRAS, 406, 1944
Wiersema, K., Levan, A.J., Kamble, A., Tanvir, N.R., Malesani, D., 2009a, GCN 9673
Wiersema, K., Tanvir, N.R., Cucchiara, A., Levan, A.J., Fox, D., 2009b, GCN 10263
Woosley, S. E. & Heger, A., 2006, ApJ, 637, 914
Xu, D., Fynbo, J.P.U., Tanvir, N.R., et al., 2009, GCN 10053
Yonetoku, D., Murakami, T., Nakamura, T., et al., 2004, ApJ, 609, 935